WEP Warwick Evans Publishing

International Journal of Mechanical and Electrical Engineering

ISSN: 3005-9615 (Print), ISSN: 3005-7132 (Online) | Volume 2, Number 1, Year 2024
DOI: https://doi.org/10.62051/ijmee.v2n1.08
Journal homepage: https://wepub.org/index.php/IJMEE/index

Research on Super-Twisting Sliding Mode Voltage Regulation Control of Electric Spring

Yaobin Wang, Tao Zhang, Pengpeng Hou

College of Electrical Engineering and Automation, Henan Polytechnic University, Jiaozuo, China

ABSTRACT

The traditional control of electric spring (ES) is too complex and lack of robustness, as well as the chattering phenomenon and control accuracy of traditional sliding mode control, a second-order terminal sliding mode control based on super twisting algorithm is proposed. In this paper, the phase plane method is used to establish the mathematical model of ES, solve the state space equation, and regard the AC power supply as a simplified error analysis. Then a second-order sliding mode controller is proposed. The controller parameters are solved to obtain the second-order sliding mode control rate, and the stability is verified. Finally, three groups of comparative simulation experiments were set up by Matlab/Simulink, and the effectiveness of the model was verified by considering the voltage mutation caused by the change of power supply and circuit parameters. Compared with the traditional control method, the proposed control strategy not only ensures the voltage stability, but also improves the control accuracy and the performance of suppressing sliding mode chattering, and has better dynamic response ability.

KEYWORDS

Electric Spring; Renewable Energy Generation; Super-twisting Algorithm; Sliding Mode Control.

1. INTRODUCTION

With the continuous development of renewable energy, the unpredictability and intermittency of new energy generation lead to power quality problems such as voltage transient rise, voltage transient drop, frequency fluctuation, etc. in the power grid [1-2]. For the power quality problems mentioned above, large power grids have a certain self-regulation ability, while isolated mini-grids can be greatly affected, and even cause harm to consumers' power equipment. Traditional reactive power compensation devices such as static reactive power compensators and static reactive power generators can regulate the grid voltage through reactive power compensation, but cannot regulate the active power. In order to better solve the problem of voltage fluctuations brought about by new energy generation, Xu Shuyuan's team at the University of Hong Kong put forward the concept of power springs in 2012, ES can make the voltage changes and energy fluctuations on the grid side transfer to non-critical loads to ensure that the critical loads operate in a stable manner, and play the role of a "spring". Changes the operation of the traditional power system, so that the relationship between supply and demand is transformed, so that the load-side consumption with the supply of renewable energy changes and changes, greatly improving the economy of power system operation.

Compared to conventional circuit compensation devices, ES has smaller capacity and better compensation performance [3-4]. And the decentralized operation of ES on the customer load side greatly improves the reliability and stability of power supply, and compared with traditional measures to mitigate fluctuations in RES supply such as controlling load switching, ES does not impede the normal use of electricity on the customer side, which to some extent improves the customer's comfort

and well-being of electricity [5]. The core structure of ES is the inverter, and the initial topology ES-1 can only realize reactive power compensation, but with the research of scholars at home and abroad in recent years, various new topologies of ES and the feasibility of ES in the aspects of frequency stabilization and power factor correction have also been confirmed [6-7]. ES initially used predominantly linear controllers, ranging from PI controllers for ES-1 [8-9] to PR controllers for ES-2 [10]. Then to various intelligent control methods, the control of ES gradually develops towards strong robustness, nonlinearity and intelligence. ES belongs to variable structure nonlinear systems, linear controllers often can not play a good effect, such as the PI controller can not be realized on the AC reference signal of the non-differential following, and the traditional linear controller parameter debugging time-consuming and laborious, so more and more nonlinear control theories have been utilized in the electric power springs, such as the smooth-mode control [11], fuzzy control [12], repetitive control [13], adaptive control [14], and so on.

Sliding mode variable structure control is a nonlinear control method, which has stronger robustness and resistance to external disturbances, as well as stronger adaptive ability compared with the traditional linear control method, and is very suitable as a controller for inverter structure [15]. However, the traditional sliding mode control is essentially a discontinuous control method, which leads to the unavoidable jitter problem, thus affecting the control accuracy and possibly even causing system oscillations. Higher-order sliding mode control has become a new control method nowadays because it can effectively suppress jitter while keeping the traditional sliding mode algorithm simple, robust and easy to implement. In practice, higher-order sliding mode control algorithms are widely used in different fields. Zhengming Li et al [16] applied the super-helix second-order sliding mode control algorithm to the maximum power tracking of photovoltaic system, which eliminates the jitter while realizing the maximum power tracking by transferring the discrete control law to the higher order so that the control quantity is continuous in time, which has a better effect compared with the traditional algorithm. David Wang et al [17] applied the second-order sliding mode control to the trajectory tracking of UAV, and Qingchao Zhang et al [18] introduced the second-order sliding mode control rate for the outer loop control link of the motor speed, which had a good control effect.

In summary, this paper proposes a second-order terminal sliding mode control method utilizing the super-helix algorithm combined with terminal sliding mode control, in response to the complexity and low robustness of the ES traditional linear control algorithm and the jitter phenomenon and control accuracy problems of the traditional sliding mode control. The single-phase ES-2 topology is used as a research object so that the ES can effectively stabilize the CL voltage when subjected to external disturbances. Finally, the feasibility and effectiveness of the technical scheme are demonstrated by Matlab/Simulink simulation experiments.

2. ES MODELING

2.1. ES Topology

Figure 1 shows the system structure of a single ES-2. The dashed box on the left shows the ES-2 circuit, which consists of a DC-side battery, an inverter and an LC low-pass filter. V_{in} denotes the DC-side battery voltage. U_g denotes the AC grid voltage. U_{es} denotes the ES output voltage. Z_{cl}, U_{cl} denote the impedance and voltage of the critical load, respectively. Z_{ncl}, U_{ncl} denote the impedance and voltage of non-critical loads, respectively. Z_t, U_t denote the line impedance and line voltage, respectively.

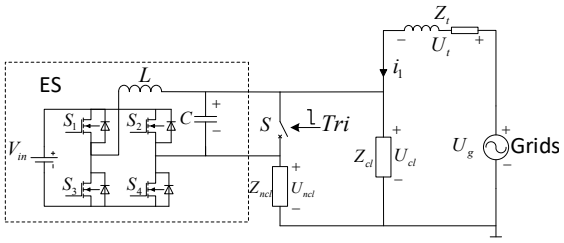

Fig 1. Single phase ES-2 system diagram

Figure 1 shows a simplified schematic of the system shown in Figure 2, it is clear that the system exists two inputs and one output, the analysis is more difficult, the general approach is to take one of the inputs as an error, this paper will be the bus inputs to the AC side of the system power supply, that is, the current As a disturbance to be dealt with.

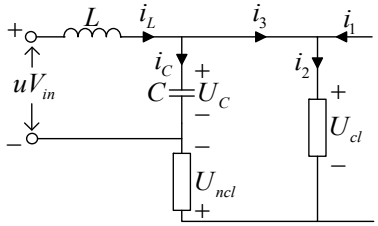

Fig 2. Simplified schematic diagram of system structure

2.2. Mathematical Model of ES

Take Fig. 3 as an object to establish a single-phase ES-2 system variable structure model, according to the circuit structure by Kirchhoff's law, using the phase plane analysis method to analyze the system, With U_{cl} and $\dot{U}_{\mathrm{cl}}$ as phase variables, the state equation can be obtained as:

$$\begin{bmatrix} \dot{U}_c \\ \ddot{U}_{cl} \end{bmatrix} = \begin{bmatrix} 0 & 1 \\ -\dfrac{1}{LC} & -\dfrac{1}{C(Z_{cl}+Z_{ncl})} \end{bmatrix} \begin{bmatrix} U_{cl} \\ \dot{U}_{cl} \end{bmatrix} + \begin{bmatrix} 0 \\ \dfrac{-V_{in}Z_{cl}}{LC(Z_{cl}+Z_{ncl})} \end{bmatrix} u + \begin{bmatrix} 0 \\ Z_{ncl}\dot{i}_1 + L\ddot{i}_1 + LCZ_{ncl}\dddot{i}_1 \end{bmatrix}, \tag{1}$$

Ignoring current i_1:

$$\begin{bmatrix} \dot{U}_{cl} \\ \ddot{U}_{cl} \end{bmatrix} = \begin{bmatrix} 0 & 1 \\ -\dfrac{1}{LC} & -\dfrac{1}{C(Z_{cl}+Z_{ncl})} \end{bmatrix} \begin{bmatrix} U_{cl} \\ \dot{U}_{cl} \end{bmatrix} + \begin{bmatrix} 0 \\ \dfrac{-V_{in}Z_{cl}}{LC(Z_{cl}+Z_{ncl})} \end{bmatrix}, \tag{2}$$

Eq. (2) where u is the power tube switching function, u∈ [-1.1], u = 1 means that only S1 and S4 conduct. u = -1 means that only S2 and S3 conduct. When the CL reference voltage U_{ref} is known, Using the error signal e=U_{ref}-U_{cl} as the new state variable, the new system state equation is:

$$\begin{bmatrix} \dot{e} \\ \ddot{e} \end{bmatrix} = \begin{bmatrix} 0 & 1 \\ -\dfrac{1}{LC} & -\dfrac{1}{C(Z_{cl}+Z_{ncl})} \end{bmatrix} \begin{bmatrix} e \\ \dot{e} \end{bmatrix} + \begin{bmatrix} 0 \\ \dfrac{-V_{in}Z_{cl}}{LC(Z_{cl}+Z_{ncl})} \end{bmatrix} u + f(x,t), \tag{3}$$

Of these:

$$F(x,t) = \ddot{U}_{ref} + \frac{1}{C(Z_{cl}+Z_{ncl})}\dot{U}_{ref} + \frac{1}{LC}U_{ref} \tag{4}$$

3. CONTROL STRATEGY

For the mathematical model of ES system in the previous section, the block diagram of the control system used in this paper is shown in Fig. 3. The control idea is as follows: when the grid voltage is stable and the ES is not put into use, the voltage sensor collects the voltage U_{cl} of the key load, at this time, the key load voltage U_{cl} is stable. Based on this voltage as the reference voltage U_{ref} of the key load when the voltage fluctuation occurs, the error is obtained and processed by the controller to output a signal to control the switching tube of the inverter system, and finally, the actual key load voltage U_{cl} is able to follow the target value U_{ref}, so that the error between the two tends to be close to 0, which in turn realizes the control objective.

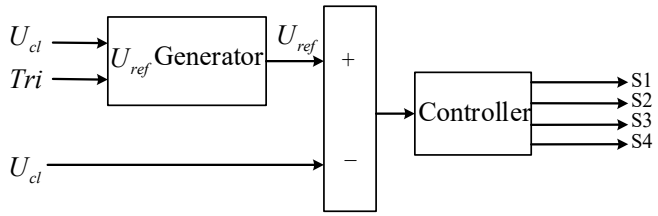

Fig 3. Control System Block Diagram

3.1. U_{ref} Generation

The structure of the reference voltage generation module is shown in Figure 4. *T*ri is the switch that controls whether ES is put into the system and is used to generate the key load reference voltage U_{ref}. When the supply side is normal and all devices work normally, the control signal *T*ri is set to 1, at this time the ES is not involved in the circuit regulation, the phase-locked loop extracts the phase of the CL voltage at this time. When the system fluctuation, need ES work, Tri set 0, then the CL voltage phase is locked by the delay module, the delay time is an integer number of frequency cycles, after that, no matter how the system changes, the CL voltage phase and amplitude is always unchanged, the phase through the sin module and the amplitude gain m, that is, the generation of the reference voltage.

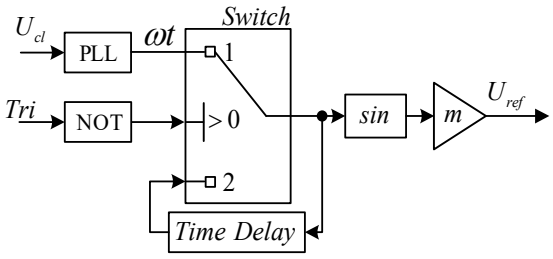

Fig 4. U_{ref} generate module structure diagram

3.2. Sliding Mold Surface Selection

Sliding mode controllers usually suffer from the singularity problem, which means that when the state of the system reaches some specific point, the derivatives of the sliding mode surface or the second-order derivatives suddenly become zero or diverge, resulting in the sliding mode controller not being able to continue to work and the control system failing. The occurrence of singular problems usually leads to instability and oscillations in the system, which seriously affects the performance and reliability of the system. To solve this problem, the non-singular terminal sliding mode control introduces a non-singular terminal condition to ensure that the sliding mode surface can smoothly transition when it reaches the target point, thus eliminating the terminal collision problem.

In order to reflect the superiority of the second-order sliding mode control, the second-order sliding mode control sliding mode surface is still chosen to be the same as the traditional sliding mode with

non-singular terminal sliding mode surface. The non-singular terminal sliding mode surface is defined as:

$$s = x_1 + \frac{1}{\beta} x_2^{p/q}, \tag{5}$$

where $\beta > 0$, p and q are positive odd and $1 < p/q < 2$.

According to Eq. (3) ES model state equation, Eq. (5) can be reduced to Eq. (6):

$$s = e + \frac{1}{\beta} \dot{e}^{p/q}, \tag{6}$$

Solving for the derivative yields:

$$\dot{s} = \dot{e} + \frac{1}{\beta} \frac{p}{q} \dot{e}^{p/q-1} \ddot{e}_{\circ} \tag{7}$$

3.3. Traditional Terminal Sliding Mode Control Law

Let s=0, s=0 Combined with Eqs. (3) (5) (6) (7), the equivalent control of terminal sliding mode can be obtained as:

$$u_{eq} = \frac{LC(Z_{cl} + Z_{ncl})}{V_{in} Z_{cl}} \left[\left(\beta \frac{q}{p} \dot{e}^{1-p/q} - \frac{1}{C(Z_{cl} + Z_{ncl})} \right) \dot{e} - \frac{e}{LC} + F(x,t) \right], \tag{8}$$

The total terminal slip mold control rate can be obtained as:

$$u = u_{eq} + u_{vss} = \frac{LC(Z_{cl} + Z_{ncl})}{V_{in} Z_{cl}} \left[\left(\beta \frac{q}{p} \dot{e}^{1-p/q} - \frac{1}{C(Z_{cl} + Z_{ncl})} \right) \dot{e} - \frac{e}{LC} + F(x,t) \right] + \text{sgn}(s)_{\circ} \tag{9}$$

Among them, u_{vss} is the switching control term, which is generally a symbolic function, and it can be seen from the control law of traditional sliding mode control that the control rate u contains a high-frequency switching term, sgn(s), which leads to the occurrence of jitter phenomenon, and the traditional sliding mode control control law requires an accurate mathematical model, which increases the amount of computation.

From Eq. (3), the affine nonlinear function of the single-input single-output system is given as:

$$\dot{x} = f(x) + bu, \tag{10}$$

Of these:

$$b = -\frac{V_{in} Z_{cl}}{LC(Z_{cl} + Z_{ncl})}, \tag{11}$$

$$f(x) = -\frac{U_{cl}}{LC} - \frac{1}{C(Z_{cl} + Z_{ncl})} \dot{U}_{cl}, \tag{12}$$

It can be seen from equation (10) that the relative order of the system is 1, which, combined with equation (3) and (7), will be substituted into, we can get:

$$\dot{s} = \dot{e} + \frac{1}{\beta} \frac{p}{q} \dot{e}^{p/q-1} \left[-\frac{1}{LC} - \frac{1}{C(Z_{cl} + Z_{ncl})} \dot{e} + \frac{V_{in} Z_{cl}}{LC(Z_{cl} + Z_{ncl})} u + F(x,t) \right], \tag{13}$$

Equation (13) can be written as:

$$\dot{s} = \sigma(t, x_1, x_2) + r(t, x_1, x_2) u, \tag{14}$$

where σ(t,x_1,x_2), r(t,x_1,x_2) are uncertain functions, $x_1 = e, x_2 = \dot{e}$ and satisfy the following boundary conditions:

$$\begin{cases} |\sigma(t, x_1, x_2)| \le \varphi; \\ 0 < K_{\min} < |r(t, x_1, x_2)| < K_{\max}, \end{cases} \tag{15}$$

The superhelix algorithm consists of two parts in the form of an algorithm:

$$\begin{cases} u = -\lambda |s|^{\alpha} \operatorname{sgn}(s) + u_1; \\ \dot{u}_1 = -\gamma \operatorname{sgn}(s), \end{cases} \tag{16}$$

To ensure that the system converges in finite time, the condition [19-20] needs to be satisfied as:

$$\begin{cases} \gamma > \dfrac{\varphi}{K_{\min}}; \\ \lambda^2 \ge \dfrac{4\varphi}{K_{\min}^2} \dfrac{K_{\max}(\gamma + \varphi)}{K_{\min}(\gamma - \varphi)}, \end{cases} \tag{17}$$

where $K_{\min}$ and $K_{\max}$ are the unknown bounds of the two generalized functions in the second-order sliding mode variable, whose values depend on the specific system, and γ , φ, $K_{\min}$, and $K_{\max}$ are constants greater than zero.

The total control rate of the superhelix algorithm can be expressed as:

$$u = -\lambda |s|^{\alpha} \operatorname{sgn}(s) - \int \gamma \operatorname{sgn}(s) dt, \tag{18}$$

To wit:

$$u = \begin{cases} -\lambda s^{\alpha} - \int \gamma dt & s > 0; \\ \lambda s^{\alpha} + \int \gamma dt & s < 0. \end{cases} \tag{19}$$

Where,s is the sliding mode variable; sgn(s) is the sign function; α, λ, γ are the adjustable control parameters, and λ, γ is greater than 0. When α is taken as 0.5, the system will maximally realize the second-order sliding mode.

Selection of Lyapunov functions:

$$V = \frac{1}{2} s^2, \tag{20}$$

Derivation of V yields:

$$\dot{V} = s\dot{s} = s(\sigma + ru) = s\sigma + sr\left(-\lambda |s|^{\alpha} \operatorname{sgn}(s) - \int \gamma \operatorname{sgn}(s) dt\right), \tag{21}$$

From equation (15):

$$\dot{V} < \sigma |s| - r \int \gamma |s| dt - r\lambda |s|^{3/2}, \tag{22}$$

From equation (17):

$$\dot{V} < -r\lambda |s|^{3/2}. \tag{23}$$

Therefore, Eq. (20) satisfies Lyapunov's stability theorem, indicating that the system is stable.

4. SIMULATION AND ANALYSIS

In order to better observe the performance of the second-order sliding-mode controller, three kinds of controllers, namely, quasi-PR controller, traditional terminal sliding-mode controller, and second-

order terminal sliding-mode controller, are set up for comparison experiments, and the other circuit parameters are kept the same except for the different controller parameter settings. The delay time in the U_{ref} generation module is 0.02s.

4.1. Parameter Setting

The parameters of the main circuit are shown in Table 1, which are identical in the comparison experiments except for the different controller parameters.

Quasi-PR (QPR) controller parameters K_p=1, K_r=450, P=0.3; Traditional terminal sliding mode (TTSM) controller parameters β=4.5×10^5, p/q=7/5, Gain=10; Second-order terminal sliding mode (STSM) controller parameters λ = 10, γ = 0.25, α = 0.5.

Table 1. Main circuit parameters

Circuit element	Value
Transmission Line Impedance	0.6 Ω+2.86 mH
Critical load Z1	40 Ω
Non-critical load Z2	4 Ω
LC filter inductor L	0.3 Ω+3.6 mH
LC filter capacitance C	100 μF
DC Side Voltage V_{in}	360 V
Effective value of U_{ref}	220 V
Transmission Line Impedance	0.6 Ω+2.86 mH

4.2. 220V Circuit Simulation Comparison Experiment

4.2.1. Change in Grid Voltage Ug

When the supply voltage is 262 V, the load operates normally, and the critical load voltage can be maintained at 220 V. The power spring does not participate in the circuit regulation at 0~0.2 s, and it is put into operation at 0.2 s. The grid voltage changes from 262 V to 301.3 V and 222.7 V, respectively, with a 15% rise and fall in 0.4 s. The power spring is not involved in the circuit regulation. Also, three different controllers: a linear quasi-PR controller, a conventional terminal sliding mode controller, and a second-order terminal sliding mode controller are used and their performances are compared by means of amplitude versus RMS variation plots in Figs. 5, 6, 7, and 8.

Experimental results show that transient perturbations were observed under linear quasi-PR control when the power spring was engaged, indicating that the ES start-up affected the voltage stability due to the effect of ES energy storage, which could be eliminated by the other two sliding mode controls. All the control systems exhibit transient oscillations when the voltage starts to vary, which is due to transient changes in the voltage, and these oscillations can also be effectively suppressed by the respective control strategies.

Comparing the performance of these three control strategies, it can be observed that at the instant of voltage change, all the three control strategies show relatively stable voltage control, in which the conventional linear quasi-PR control voltage transient rise and fall change after the amplitude of the first cycle of the first cycle of the error of about +8.5V and -5V, respectively, and after the voltage change to reach a steady state after 0.07s, the steady state values of 220.2V and 220.05V, respectively. The steady state waveforms have tiny fluctuations. For the traditional terminal sliding mode control and the second-order terminal sliding mode control, the amplitude of the first cycle after the voltage transient rise and fall changes can reach the reference value of 311V, and the steady state can be reached after 0.02s after the voltage changes, in which the steady state error of the traditional terminal sliding mode control can be controlled at ±0.2V, and that of the second-order terminal sliding mode control can be controlled at ±0.1V, and the steady state waveforms are more smooth. smooth.

The simulation experiments show that the traditional quasi-PR control in power spring voltage stabilization control has a slow response time, moderate overshooting, transient oscillations and minor steady-state fluctuations; the traditional terminal sliding-mode control exhibits relatively stable voltage control during voltage increase and decrease, with slight deviations during the transition process, and exhibits small overshooting, fast adjustment speed and good steady-state performance; The second-order terminal sliding mode control exhibits excellent voltage control performance with minimal steady-state error, fast response time and smooth waveform transition, and it effectively solves the overshooting and oscillation problems existing in the traditional control strategy and improves the steady-state control accuracy of the terminal sliding mode control.

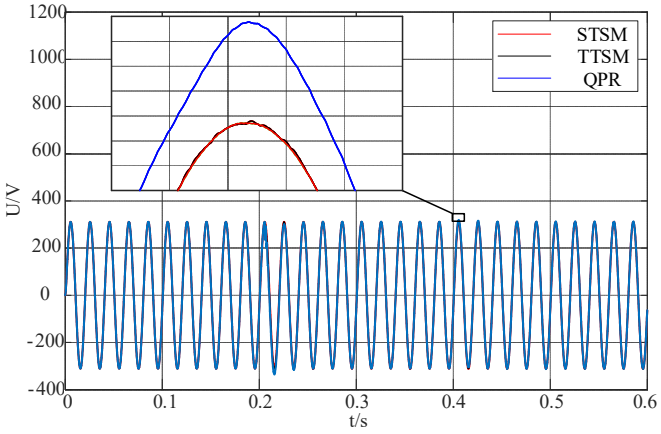

Fig 5. The amplitude changes when the voltage rises temporarily

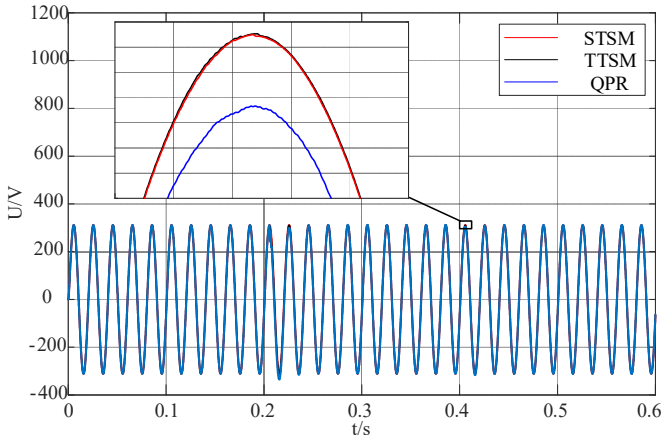

Fig 6. The amplitude changes when the voltage decrease temporarily

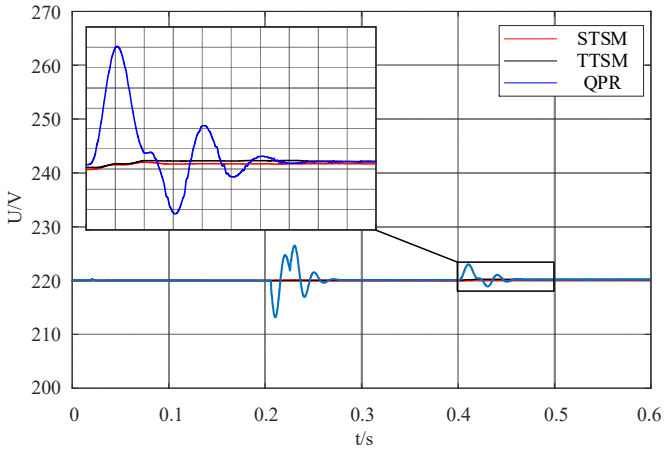

Fig 7. The RMS value changes when the voltage rises temporarily

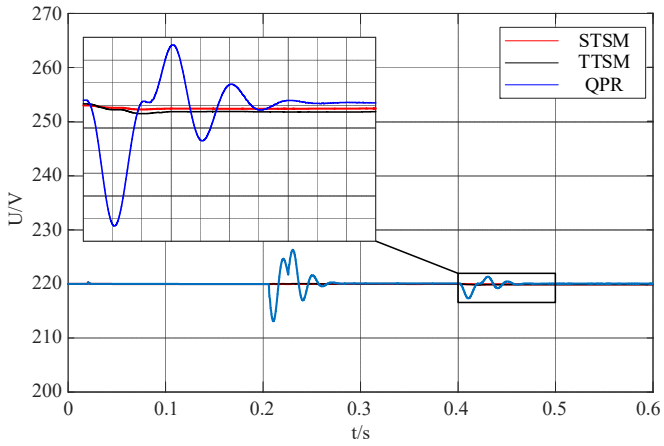

Fig 8. The RMS value changes when the voltage decrease temporarily

4.2.2. Loaded Z_{cl} Mutation

When U_g is 262V, the key load is 40Ω stable operation, ES is put into the system at 0.2s, 0.2-0.3s, after a short period of oscillation and overshooting, the voltage is stabilized at 220V, and the size and properties of the key load are changed at 0.3s, to observe the change of U_{cl} under the three control modes, and the change of loads is shown in Table 2, and the change of U_{cl} when the key loads are changed suddenly is shown in Fig. 9 shows.

Table 2. Load variation table

Time	CL Resistance
0.3s~0.4s	40Ω
0.4s~0.5s	80Ω
0.5s~0.6s	20Ω
0.6s~0.7s	40Ω+0.01H
0.7s~0.8s	40Ω+100μF

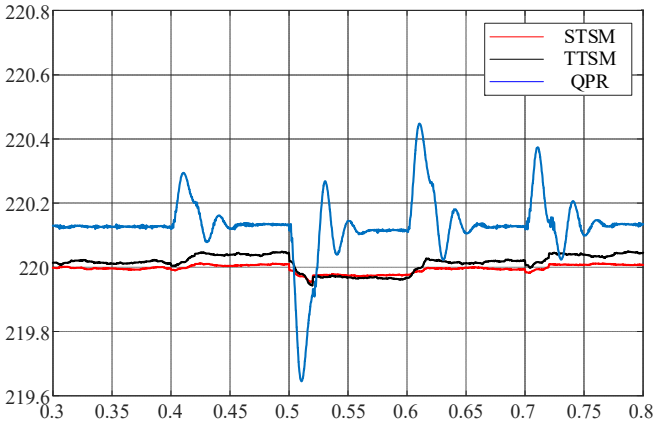

Fig 9. Changes in U_{cl} RMS value during critical load mutations

According to the results shown in Fig. 9, the variation of RMS values under different load cases exhibits the following characteristics: all three control methods are able to effectively maintain the stability of the load voltage during sudden load changes. However, there are obvious differences between the various control strategies. The conventional PR control exhibits large fluctuations and overshoots, which means that the voltage experiences large fluctuations when the load changes and

there is a period of overshoots before reaching the steady state. The conventional terminal sliding mode control has a slightly higher steady state error although it is more stable. In contrast, the second-order sliding mode control can respond quickly when the critical load undergoes a sudden change and is able to essentially stabilize the voltage at the reference value of 220V with a smoother waveform, exhibiting higher control accuracy. These results emphasize the excellent performance of the second-order sliding mode control in the face of load variations.

4.3. Comparative Experiments on Jitter and Tracking Performance Simulation

In order to verify the superiority of the second-order terminal sliding mode control in suppressing sliding mode vibration, simulation and comparison experiments with the traditional terminal sliding mode control are carried out. Figs. 10 and 11 show the comparison of the control law u of the traditional terminal sliding mode control and the second-order terminal sliding mode control in the steady state after the ES input and the voltage transient change, respectively, and Figs. 12 and 13 show the comparison of the voltage tracking error e of the traditional terminal sliding mode control and the second-order terminal sliding mode control in the steady state after the ES input and the voltage transient change in the steady state after the ES input and the voltage transient change, respectively.

As can be seen from FIG. 10, FIG. 11, due to the presence of the discontinuous high-frequency switching term sgn(s), the control law u of the conventional terminal sliding mode controller shows high-frequency jittering of the waveforms after the ES is put in and after the voltage undergoes a transient rise change, whereas the control law u of the second-order terminal sliding mode controller can act the discontinuous high-frequency switching term into the second-order inverse, and the control quantities are continuous in time, thus suppressing jittering.

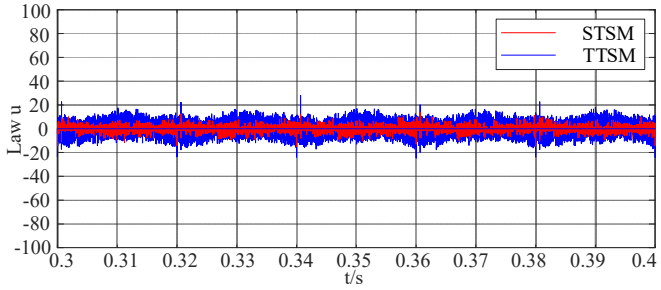

Fig 10. Change in control law u after the introduction of ES

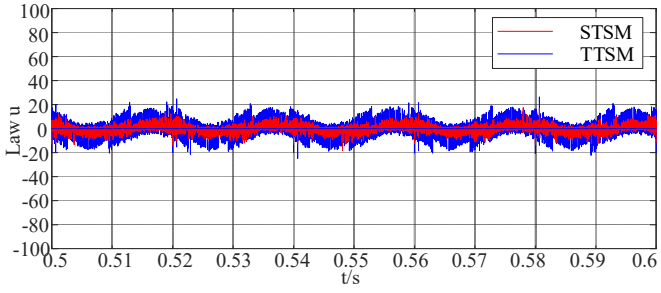

Fig 11. Change in control law u after the voltage transient rise

From Fig. 12, Fig. 13, it can be seen that the voltage tracking error of the conventional terminal sliding mode control can be up to about 1.5V and 1.8V at steady state after the ES is put in and after the voltage undergoes a transient rise and change, whereas the voltage tracking error of the second-order terminal sliding mode controller is up to only about 0.4V and 0.8V at steady state. This shows that the second order terminal sliding mode control has higher voltage tracking accuracy under the same conditions.

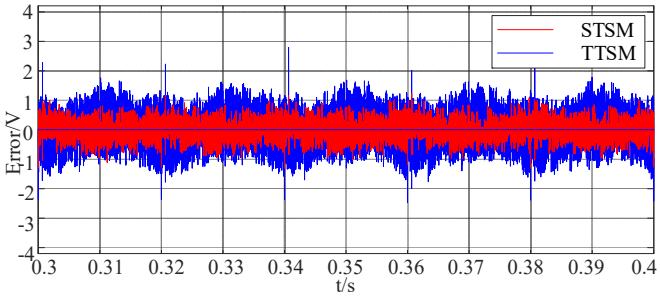

Fig 12. Voltage error *e* after the introduction of ES

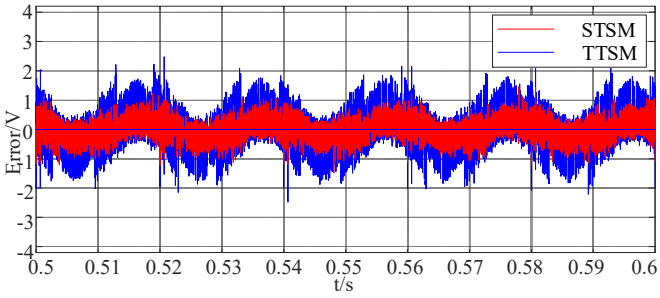

Fig 13. Voltage error *e* after the voltage transient rise

5. CONCLUSION

Aiming at the shortcomings of the traditional sliding mode controller with insufficient control accuracy and jitter vibration phenomenon, this paper introduces a second-order terminal sliding mode controller based on the super-helix algorithm into the control system of the power spring, and the following conclusions are drawn from the comparison of the quasi-PR control, the traditional terminal sliding mode control, and the second-order terminal sliding mode control through the simulation experiments in MATLAB:

(1) Through the comparative simulation simulation under grid fluctuation, sudden change of CL load, it is found that the second-order sliding mode controller has better dynamic and static characteristics compared with the traditional sliding mode controller, and at the same time solves the oscillation and overshooting problems of the linear controller.

(2) The second-order sliding mode controller is simple to design, and the second-order sliding mode controller based on the super-helix algorithm only needs to know the information of the sliding mode surface s, and does not need an accurate mathematical model and other information.

(3) The second-order sliding mode control transfers the discontinuous high-frequency switching term sgn(s) from the control rate *u* to the first-order derivative of *u*. The output control signal is continuous, which essentially optimizes the jitter phenomenon.

(4) The problem of the second-order sliding mode is that the parameters of the control rate are difficult to determine, and it is necessary to know the boundaries of the system's uncertainty, and the boundary conditions given in the paper are sufficient conditions, which have a certain degree of conservatism, and at the same time, the second-order sliding mode algorithm is only applicable to the case of the system's relative order $r \leq 2$.

The next work will consider how to improve the adaptive capability of the second-order sliding mode control, consider combining other optimization algorithms with the second-order sliding mode control, or consider optimizing and improving the ES topology to improve the adaptive capability of the ES from the fundamental point of view.

REFERENCES

[1] LEE C K, CHAUDHURI B, HUI S Y. Hardware and Control Implementation of Electric Springs for Stabilizing Future Smart Grid with Intermittent Renewable Energy Sources[J/OL]. IEEE Journal of Emerging and Selected Topics in Power Electronics, 2013, 1(1): 18-27.

[2] WANG Q S. Research on Several Key Technologies of Power Springs. [D]. Nanjing: Southeast University, 2017.

[3] LUO X, AKHTAR Z, LEE C K, et al. Distributed Voltage Control with Electric Springs: Comparison with STATCOM[J/OL]. IEEE Transactions on Smart Grid, 2015, 6(1): 209-219.

[4] CHE X, WEI T, HUO Q, et al. A general comparative analysis of static synchronous compensator and electric spring[C/OL]//2014 IEEE Conference and Expo Transportation Electrification Asia-Pacific (ITEC Asia-Pacific), Beijing, China. 2014

[5] MOHSENIAN-RAD A H, LEON-GARCIA A. Optimal Residential Load Control With Price Prediction in Real-Time Electricity Pricing Environments[J/OL]. IEEE Transactions on Smart Grid, 2010, 1(2): 120-133.

[6] YANG Y, TAN S C, HUI S Y. Voltage and frequency control of electric spring based smart loads[C/OL]//2016 IEEE Applied Power Electronics Conference and Exposition (APEC), Long Beach, CA, USA. 2016.

[7] SONI J, PANDA S K. Electric spring for voltage and power stability and power factor correction[C/OL]//2015 9th International Conference on Power Electronics and ECCE Asia (ICPE-ECCE Asia), Seoul, South Korea. 2015.

[8] AREED E F, ABIDO M A. Design and dynamic analysis of Electric Spring for voltage regulation in smart grid[C/OL]//2015 18th International Conference on Intelligent System Application to Power Systems (ISAP), Porto, Portugal. 2015.

[9] LEE C K, TAN S C, WU F F, et al. Use of Hooke's law for stabilizing future smart grid — The electric spring concept[C/OL]//2013 IEEE Energy Conversion Congress and Exposition, Denver, CO, USA. 2013.

[10] CHENG M, WANG Q S, ZHANG J Z. Theoretical Analysis and Controller Design of Power Springs. [J] Proceeding of the CSEE, 2015,35(10):2436-2444.

[11] YIN F, WANG C, WANG W. Adaptive Sliding-Mode Control for Electric Spring in Microgrids with Distributed Renewable Energy[J/OL]. Energies, 2022: 4842.

[12] LV G Q, XU W M, WANG P Y. Power Spring Con-trol Strategy Based on Variable Universe Fuzzy PI Adaptive Contro. [J] Power System Automation,2020,44(18):172-178.

[13] ZHENG Z, ZHANG Q, ZHANG T, WANG Y S, et al. Research on Power Spring Based on Repetitive Control. [J] Journal of Henan University of Technology (Natural Science Edition),2021,40(03):106-112.

[14] ZHANG T, LU C, ZHENG Z. Adaptive Fuzzy Controller for Electric Spring[J/OL]. European Journal of Electrical Engineering, 2020, 22(3): 233-239.

[15] ZHANG L, QIU S S. Analysis and Experimental Study of Sliding mode control Inverter. [J] Proceeding of the CSEE, 2006,26(3): 59-63.

[16] LI Z M, SHAN X C, XU P K. Realization of Photovoltaic MPPT Based on Super Spiral Sliding mode control. [J] Power System Protection and Control,2018,46(21):32-37.

[17] WANG D W, GAO X F. Design of sliding mode trajectory tracking controller for quadrotor uav.[J] Electro Optics and Control, 2016, 23(07): 55-58+63.

[18] ZHANG Q C, MA R Q, HUANGFU Y G, et al. Design and Research on the Second Order Sliding mode control Control Law of Super Twisting Algorithm for Motor Speed Link. [J] Journal of Northwestern Polytechnical University, 2016,34(04):669-676.

[19] LEVANT A. Universal single-input-single-output (SISO) sliding-mode controllers with finite-time convergence [J/OL]. IEEE Transactions on Automatic Control, 2001, 46(9): 1447-1451.

[20] LEVANT A. Sliding order and sliding accuracy in sliding mode control[J/OL]. International Journal of Control, 1993, 58(6): 1247-1263.